Protons and Deuterons Ejected from Nuclei by 90-Mev Neutrons*

JAMES HADLEY AND HERBERT YORK
Radiation Laboratory, Department of Physics, University of California, Berkeley, California
(Received February 16, 1950)

The angular and energy distributions of the fast charged particles emerging from nuclei bombarded by 90-Mev neutrons have been investigated. The results indicate that the nature of the collision process is determined predominantly by interactions of the bombarding particle with single nucleons rather than with the struck nucleus as a whole: angular distributions are found to be peaked in the forward direction for all emergent particles, the degree of peaking increasing with energy. Deuterons are found to be more concentrated in the forward direction than are protons. In the case of carbon, particles traveling in the forward direction with energies greater than 20 Mev consist of 60 percent protons, 36 percent deuterons, and about 4 percent tritons.

I. INTRODUCTION

THE inelastic processes which take place when nuclei are bombarded by nucleons with energies up to a few tens of Mev, or by alpha-particles with energies up to 50 Mev, are well described by Bohr's theory of the compound nucleus,[1] involving excitation of the whole nucleus with subsequent photon or particle emission. The energy of the incident particle is at first distributed among all of the constituent particles of the nucleus; a time long with respect to transit times of nucleons within the nucleus elapses before a sufficient amount of this energy chances to be concentrated in one nucleon to enable it to escape. Consequently the anisotropy contributed by the directed motion of the incident particle is almost entirely lost by the time of emission, and the emitted particle may take any direction with equal probability.

Since a basic assumption of this theory is that the mean free path for nucleons in nuclear matter is small compared with the dimensions of the nucleus, it may be expected to become less applicable with increase in energy of the bombarding particle and resulting decrease in nucleon-nucleon cross sections.

The total 90-Mev cross section measurements of Cook *et al.*[2] and the total and inelastic cross section measurements of DeJuren and Knable[3] and of Bratenahl *et al.*[4] indicate that loss of validity of the Bohr theory may be expected at that energy. Those measurements show a considerable transparency for 90-Mev neutrons, particularly in the case of light nuclei, demonstrating that the mean free path for these neutrons in nuclear matter is no greater than the order of size of the nuclear diameter. Fernbach, Serber, and Taylor[5] have calculated from data of this type that the mean free path is 4.5×10^{-13} cm, and a value close to this was previously estimated by Goldberger.[6] The mean free path is the same in all nuclei because of the constant density of nuclear matter.

Qualitatively then, the sequence of events in an inelastic collision at these high energies would be expected to take the following course (similar analyses pertaining to high energy cosmic-ray stars have been given by Heisenberg[7] and by Bagge[8]). The impinging neutron strikes a nucleon in the nucleus, imparting to it some of its energy; the struck nucleon is most likely to be a proton because the $n-p$ cross section is probably several times larger than the $n-n$ cross section.[9]

There are at this point two fast nucleons moving in the nucleus. They may, because of their high energy, either collide with additional particles or escape from the nucleus without further interaction. Thus the immediate emission of one or more fast particles may occur, followed by the formation of a relatively long-lived compound nucleus of the type described by Bohr. The fast secondaries may be charged or uncharged without prejudice, because of the relative smallness of the Coulomb barrier. Furthermore, the direction of emission of the secondaries should be correlated with that of the impinging neutron in roughly the same way as in $n-p$ scattering, where particles of high energies emerge in the forward direction and those of low energies emerge at wide angles.

Detailed quantitative predictions along this line have been given in Goldberger's paper in which he has taken into account such factors as the internal motion of the nucleons in the nucleus and the effect of the exclusion principle in a nuclear system considered as a degenerate Fermi gas.

The object of the present work was to make an experimental investigation of the high energy charged secondaries. The nuclei investigated were carbon, copper and lead. The observed phenomena do not closely agree with Goldberger's analysis, but do follow the general features outlined above except for one important

* This work was performed under the auspices of the AEC.
[1] N. Bohr, Nature **137**, 344 (1936).
[2] Cook, McMillan, Peterson, and Sewell, Phys. Rev. **72**, 1264 (1947).
[3] J. DeJuren and N. Knable, Phys. Rev. **77**, 606 (1950).
[4] Bratenahl, Fernbach, Hildebrand, Leith, and Moyer, Phys. Rev. **77**, 597 (1950).
[5] Fernbach, Serber, and Taylor, Phys. Rev. **75**, 1352 (1949).
[6] M. L. Goldberger, Phys. Rev. **74**, 1269 (1948).
[7] W. Heisenberg, Leipziger Berichte **89**, 369 (1937).
[8] E. Bagge, Ann. d. Physik **37**, 535 (1941).
[9] This fact is based primarily on statistical considerations; *i.e.*, $n-p$ scattering can take place in both singlet and triplet states for all values of l; $p-p$ scattering only in singlet states for even values of l. See for example reference 6.

difference. This difference lies in the comparatively large observed yields of secondary deuterons and tritons, which had not been predicted. Observations of the latter particles were made simultaneously and reported by Bradner[10] (photographic plates), Brueckner and Powell[11] (cloud chamber), and one of the authors.[12] High energy deuterons have also been observed among the fragments from cosmic-ray stars.[13]

II. GENERAL EXPERIMENTAL METHOD

1. Requirements

In this experiment we are concerned with measuring the angular and energy distributions of a mixture of several types of particles all of which have energies ranging from about 20 Mev to 100 Mev. The procedure

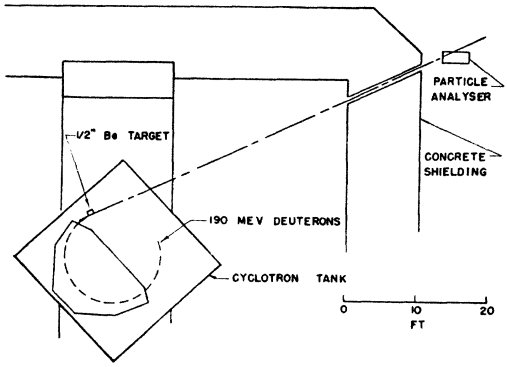

FIG. 1. General arrangement of apparatus.

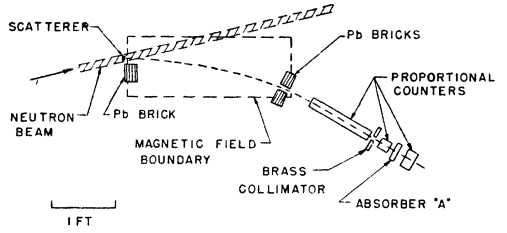

FIG. 2. Schematic diagram of particle analyzing system.

used is to measure the energy spectra at each of a series of angles.

For a known type of particle (i.e., proton, deuteron, or triton in the present case) the energy can be determined by a measurement of its $H\rho$, range, or specific ionization; conversely, for a particle of known energy the type can be determined by any one of these three measurements. In the present case it is necessary to measure simultaneously any two of the above quantities in order to determine both the type and energy of an observed particle.

[10] H. Bradner, Phys. Rev. **75**, 1467 (1949).
[11] K. Brueckner and W. Powell, Phys. Rev. **75**, 1274 (1949).
[12] H. York, Phys. Rev. **75**, 1467 (1949).
[13] Morand, Cüer, and Moucharafyeh, Comptes Rendus **226**, 1008 (1948); C. F. Powell and L. Leprince-Ringuet, Cosmic Ray Conference, Bristol, (1948).

2. Method Used

The measurements to be described here were made with $H\rho$-specific ionization combination, which makes possible the highest degree of resolution between types of particle. The $H\rho$ of the observed particles was fixed by requiring that they follow a fixed orbit in a magnetic field. The particles were then sorted according to specific ionization by passing them through a proportional counter connected to a pulse height analyzer. Protons, deuterons and tritons could be distinguished as groups of counts registered at three different levels in the pulse height analyzer. As an extra check on the results simultaneous range measurements were made in a few cases.

3. Arrangement of Components

Figures 1 and 2 show schematically the experimental arrangement used. The various components will be discussed in detail in Section III.

Neutrons of 90-Mev energy are produced by the stripping process[14] when 190-Mev deuterons strike a $\frac{1}{2}$ inch beryllium target in the 184-inch synchrocyclotron. These neutrons are collimated by a steel tube passing through the concrete shielding which surrounds the cyclotron. A neutron beam of rectangular cross section, 1 inch and $1\frac{1}{2}$ inches on the sides, emerges from this tube, and passes between the poles of the particle analyzing magnet, placed about 6 feet from the exit end of the collimator. A scatterer is placed in the beam where it enters the magnet, and a slit defined by lead bricks is placed at the other end of the magnet. A counter telescope consisting of three proportional counters is placed as shown, about 20 inches beyond the slit. Thus the charged secondaries from the scatterer travel along a circular path between the target and the slit, and along a straight path from the slit through the counters. The radius of curvature of the circular orbit is measured directly, and checked by range measurements to be described later.

III. APPARATUS

1. Counter System

The first of the three counters in the telescope is used to determine the specific ionization of the particles; the other two, which are placed in electrical coincidence with the first, are used to eliminate the large number of unwanted pulses produced in the first tube by particles entering from random directions. The ionization produced in the first tube is measured by means of a ten-channel pulse height analyzer. Absorbers can be placed in position A (Fig. 2), permitting a range measurement which can be used as an additional check on the nature of the radiation detected.

In the energy region of interest here the specific ionization is quite small. For this reason the first tube

[14] R. Serber, Phys. Rev. **72**, 1007 (1947).

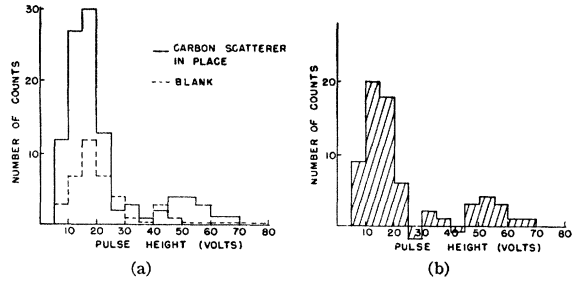

FIG. 3. Typical pulse-height histograms. (a) Counts from carbon scatterer and from blank; (b) Carbon-blank difference.

was made rather long (10 inches). This design also aids in reducing the importance of end effects in producing non-uniformity of pulse heights. The diameter of the first and second tubes is two inches, and that of the third tube about 4 inches. This increase in diameter was used in order to diminish loss of particles from scattering in the absorber sometimes placed at A, between the second and third tubes. The gas in the counters consists of 97 percent argon and 3 percent carbon dioxide, at a total pressure of about 1.1 atmospheres.

Various investigations of the operating characteristics of the first counter were made by placing a polonium alpha-gun inside in such a way as to emit alpha-particles either along a line parallel to the collecting wire or perpendicular to it. The gas amplification and the rate of change of gas amplification with collecting voltage (namely by a factor of two per hundred volts) were found to agree satisfactorily with results given by Diven and Rossi.[15] The pulse-height distribution produced by the alpha-particles consisted of a peak with a half-width of about 6 percent of the average pulse height, plus a low pulse height tail. The tail is presumably due to alphas which hit the walls of the counter before stopping, or which have suffered scattering collisions in the gun.

2. Magnet

The dimensions of the region of effective field in the magnet are 12 inches by 30 inches by $1\frac{3}{4}$ inches. The field can be adjusted to any value up to 15,000 gauss, and can be held constant to about $\frac{1}{2}$ of one percent, which corresponds to an energy variation of one percent.

3. Scatterers and Slits

The scatterers are carbon, copper and lead rectangles three inches long and one-half inch wide. They are placed in the beam with the long dimension vertical, and with the three by one-half inch face normal to the direction of emission of the particles being studied. The scatterer thus subtends the entire beam vertically, but only a small portion of it horizontally.

The thickness of the scatterers in the direction of the emitted particles under study is determined by a compromise between maximum secondary particle yield and minimum energy loss in the scatterer. The value chosen was $\frac{1}{8}$ inch for all three elements.

The first slit (Fig. 2) is formed by two lead bricks $\frac{1}{2}$ inch apart in the magnet gap near one edge. A second slit, about the same width, consists of a pair of brass plates placed between two of the proportional counters.

4. Electronics

The electronic equipment consists of two parts: a set of preamplifiers, amplifiers, and coincidence gate forming units built under the direction of H. Farnsworth, and a pulse-height analyzing system designed by Dexter and Sands[16] at the Los Alamos Scientific Laboratory, and built, with some modifications, by W. Goldsworthy and C. Wiegand at the Radiation Laboratory.

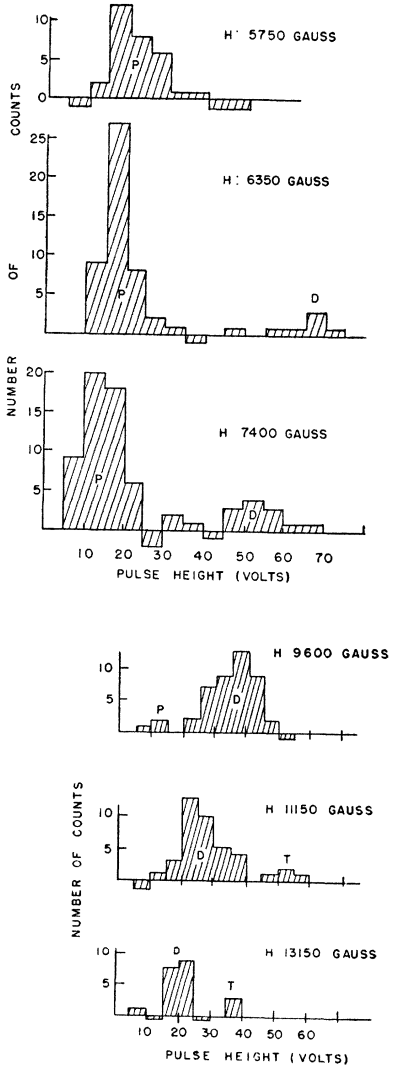

FIG. 4. Set of pulse height histograms for various magnetic fields showing proton (P), deuteron (D), and triton (T) peaks.

[15] B. C. Diven and B. Rossi, LADC-148, Los Alamos, (1944), (unpublished).

[16] E. Dexter and M. Sands, LADC 414, Los Alamos, (unpublished).

5. Monitor

The monitor consists of a boron trifluoride filled proportional counter which is inserted in the concrete cyclotron shielding a few inches from the high energy neutron collimating hole. High energy neutrons striking the steel collimator are inelastically scattered and in addition produce a number of secondary neutrons. Many of each enter the concrete, are moderated, and produce counts in the slow neutron sensitive monitor.

IV. NEUTRON BEAM

The neutron beam, produced and collimated as described in Section II, has a considerable energy spread. The spectrum as measured experimentally by Hadley *et al.*[17] and Brueckner *et al.*[18] in connection with $n-p$ scattering experiments show a peak with a maximum at about 90 Mev, and a half-width of 25 to 30 Mev. Figure 3 of reference 17 shows the spectrum as given by Hadley *et al.*; the solid curve is the spectrum predicted by the theory of Serber.[14]

As described above, the beam is collimated to a rectangular cross section measuring 1 inch vertically and $1\frac{1}{2}$ inches horizontally. By placing a long copper bar in the neutron beam in such a way as to shield the scatterer from the direct beam of collimated neutrons, we have found that less than one percent of the effects reported in this paper are produced by neutrons other than those coming through the collimating hole.

V. DATA

Figure 3a shows the pulse-height distribution obtained in a 300 second run using a scattering angle of $\theta=0°$, a field of 7400 gauss, $\rho=60$ inches, and the carbon scatterer (solid curve), together with the distribution obtained with no scatterer in place (dashed curve), for the same monitor count. Figure 3b shows the difference between these two and is thus the pulse-height distribution for particles originating in the carbon. It can be seen that the pulses fall into two groups, one of which has an average pulse height three times as large as the other. With these values of H and ρ the lower peak should consist of 63-Mev protons and the upper peak of 31.5-Mev deuterons. To check this, a carbon absorber whose thickness was equal to the range of a 45-Mev deuteron (and hence a 34-Mev proton) was placed between the second and third counters. It was then observed that the upper peak disappeared entirely while the lower peak was unaffected within the statistical accuracy.

This check was used in a number of instances in which one of the peaks was so small that its origin was somewhat doubtful, as in the case of the very small number of tritons found at high values of magnetic field. In addition, since the radius of curvature defined by the slit system is quite sensitive to the position of the slits and scatterer, it was felt that a careful determination of the range distribution of the protons should be made for some value of the magnetic field. This was done, and was found to confirm the average energy expected from geometrical considerations. The range distribution corresponded to a bell-shaped energy distribution with a half-width of about 13 percent of the average energy. Because of the relation

$$\Delta E/E=2\Delta\rho/\rho,$$

this energy resolution of 13 percent holds for all particles.

Figure 4 shows several histograms of the type presented in Fig. 3, taken at 0° scattering angle for a series of different values of magnetic field. The first graph shows the distribution obtained using a field of 5750 gauss. The duration of the run was 300 seconds, as in all the succeeding cases, for both the "scatterer in" count, and the background count. The monitor during this time recorded 86×64 slow neutron counts. At this value of magnetic field only one group of particles is seen, corresponding to 38-Mev protons. The 19-Mev deuterons which would have the same $H\rho$ are not able to penetrate all of the absorbing material along their potential path, such as the air and the counter windows. The succeeding graphs show the distributions obtained at the indicated values of H. The graphs are arranged in order of increasing H and therefore increasing energy of the particles. The proton peak can be seen moving steadily to lower values of pulse height since the specific ionization decreases with increasing energy. The first deuteron peak appears at 6350 gauss and corresponds to a deuteron energy of 23 Mev. At very high magnetic fields the protons are seen to disappear, and a new small peak to the right of the deuterons comes into existence. From its position, and from absorption measurements, this peak is ascribed to tritons.

Such histograms were obtained for 14 values of H, during each of three runs. Similar sets of data were obtained at 12°, 25°, and 45°.

VI. REDUCTION OF DATA AND DETERMINATION OF ABSOLUTE CROSS SECTIONS

1. Definition of Terms

The ultimate goal of this experiment is to determine the differential cross sections for the production of secondary charged particles of energy E at various angles θ. These cross sections will be denoted as $d\sigma_p(\theta, E)/d\Omega dE$ (abbreviated as $d\sigma_p$) where the subscript p stands for protons, and d and t for deuterons and tritons respectively. Because of the thickness of the targets and the finite acceptance interval of the slit system, the cross sections are not measured at single energies; instead their average values between two energy limits E_1 and E_2 are found. The above symbol will be understood as referring to such an average value.

[17] Hadley, Kelly, Leith, Segrè, Wiegand, and York, Phys. Rev. **75**, 351 (1949).
[18] Brueckner, Hartsough, Hayward, and Powell, Phys. Rev. **75**, 555 (1949).

Let us characterize the mean energy of the particles accepted by the magnet as E_m, and the width of the energy acceptance interval as ΔE. Then for a scatterer of infinitesimal thickness, E_1 and E_2 are $E_m-\frac{1}{2}\Delta E$ and $E_m+\frac{1}{2}\Delta E$ respectively, and

$$d\sigma_p=N_p/n_cN_n\Delta\Omega\Delta E,$$

where N_p=total proton count, N_n=total number of incident neutrons, n_c=carbon atoms/cm² in the target, and $\Delta\Omega$=solid angle presented to scatterer by slit system. Since, $\Delta E/E_m=2\Delta\rho/\rho$, and $\Delta\rho/\rho$ is a constant, $d\sigma_p$ may also be written $d\sigma_p=k(N_p/ME_m)$, where M=monitor count. The constant k contains several factors which are either difficult to determine absolutely or not well defined. It is therefore evaluated indirectly by integrating numerically, adding the various relative $d\sigma$'s involved, and setting this sum equal to the total cross section for these processes, which is in turn measured absolutely by a method to be described below.

In the case of a thick target both ΔE and the value of E_2 must be modified, because of energy loss suffered by particles in passing from their point of origin in the target to the face of the target. The energy interval E_2-E_1, over which the average value of $d\sigma$ is measured, becomes greater than the interval determined by the slit system alone. Further, ΔE, the energy interval at the point of origin corresponding to the energy interval of emergent particles which will be accepted by the slit system, depends upon the depth within the scatterer at which the particles originate, and must thus be averaged over the thickness of the scatterer. The calculation of these effects by means of range-energy curves is straightforward but tedious. The results have been used in preparation of the data.

2. Absolute Cross Section

The absolute cross sections for producing all secondary particles at a given angle θ were measured using an experimental arrangement identical to that used in the 90-Mev $n-p$ scattering experiments of Hadley *et al.*[17] The arrangement is given in Fig. 5. The location of the apparatus with respect to the cyclotron and collimating system was the same as in the part of the experiment done with the magnet.

The monitor used was a bismuth fission chamber, which is sensitive only to high energy neutrons.

The scatterers were 1″×2″ pieces of carbon (480 mg/cm²), copper (713 mg/cm²), lead (910 mg/cm²), and polyethylene (C_nH_{2n}) (420 mg/cm²). These thicknesses were chosen so that a high energy particle would lose the same amount of energy in passing through each target.

The polyethylene and carbon scatterers were bombarded first, with an absorber placed between the scatterers and counters such that a proton of energy 66 ($\cos^2\theta$) Mev originating at the center of the scatterer would just reach the end of its range upon entering the last counter. The difference between polyethylene counts per monitor count and carbon counts per monitor count is taken, giving the number of protons originating in $n-p$ collisions per monitor count. Use of the absorber mentioned above ensures that no protons recoiling from collisions with neutrons of energy less than 66 Mev will be counted. This is the same lower energy limit as that used in the 90-Mev $n-p$ scattering experiments, and we have, consequently, using the value of $\sigma_{n-p}(\theta)$ measured in that experiment, a direct proportion between number of scattered particles per

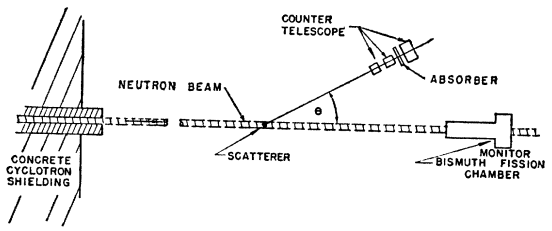

FIG. 5. Arrangement of apparatus for determining absolute cross sections.

bombarded nucleus per monitor count and the differential cross section for producing those particles.

If we are to count particles produced by neutrons of energy less than 66 Mev, the constant of proportionality must contain the factor N'/N, the ratio of the total number of effective neutrons in the beam to the number of neutrons of energy greater than 66 Mev. The carbon, copper, and lead scatterers are bombarded without the use of an absorber. Their thicknesses are such that the energies of particles originating at the scatterer center and just able to penetrate the last counter will be 20 Mev for protons, 27 Mev for deuterons, and 33 Mev for tritons. Because of the highly endothermic nature of the reactions involved, and because the cross sections for reactions of this kind typically are quite low at energies immediately above the threshold values, we can assume the lower energy limit of neutrons effective in producing observed particles to be not lower than about 50 Mev. Thus the factor N'/N above will be, at the greatest, equal to the ratio of number of neutrons of $E>50$ Mev to number of neutrons of $E>66$ Mev, or about 1.1. It may very probably be practically unity, and is taken so in the calculations of our results.

The quantities measured by this procedure are of the form

$$\sum(\theta)=[\sigma_{p>20}(\theta)+\sigma_{d>27}(\theta)+\sigma_{t>33}(\theta)],$$

where $\sigma_{p>20}(\theta)$ is the differential cross section for the production of protons of energy greater than 20 Mev at an angle θ to the direction of the incident neutrons, and so on.

Figure 6 is a plot of the results obtained. It gives the values of $\sum_c(\theta)$, $\sum_{cu}(\theta)$, and $\sum_{pb}(\theta)$ for angles ranging from 6° to 135°.

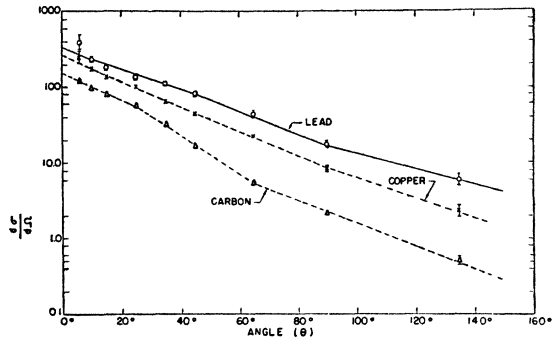

FIG. 6. Angular dependence of differential cross sections for production of secondary particles with ranges greater than 460 mg/cm² of carbon.

VII. FINAL RESULTS

1. Form

Data of the type described in Section V were obtained using carbon, copper, and lead scatterers, at angles of 0°, 12°, 25°, and 45° to the neutron beam. These data were analyzed using the methods described in Section VI to find the relative differential cross sections for each type of particle as a function of energy at each angle. A comparison with the values of $\sum(\theta)$ found by the procedure described in that section then provided absolute values for these cross sections. The final results are presented in graphical form in Figs. 7, 8, and 9.

The triton cross sections and some of the deuteron cross sections found are not plotted individually, but their average values over wide energy intervals are shown. The reason for this is that in each case the range of energies to which $d\sigma$ applies is so large, and so overlaps the neighboring values, that no spectral details could be seen.

Only in the case of the 0° carbon observations were any counts obtained which could with any real certainty be attributed to tritons. In that case they contributed 4 percent of the total cross section. Their contribution in all other cases is probably less than one percent.

2. Discussion of Error

The probable errors include only the expected statistical fluctuations in the relative values of the cross sections, and do not include the additional errors which can arise in the determination of the absolute scale. This latter error is probably of the order ±25 percent, and includes, besides the usual statistical factors, which are, in fact, quite small, two other factors. These are the uncertainty of the absolute value of the differential $n-p$ cross section involved in the calculations of the absolute cross sections, and the uncertainty involved in the numerical integration of the plots of the relative differential cross sections.

The case of the data at 0° deserves special attention in regard to these errors, for at that angle the absolute cross section for producing the secondaries was not measured at all. It can be seen in Fig. 6 that the cross sections at those points at which they were measured (6°, 10°, 25°, etc.) fall quite well on an exponential curve. This curve was extrapolated to 0°, and the extrapolated value was used in normalizing the 0° relative cross sections. This extrapolation is probably valid, since, as will be seen later, theoretical considerations indicate that there should be no marked singularities in the forward direction.

3. Total Cross Sections

In order to obtain total cross sections for the production of protons and deuterons having ranges in carbon

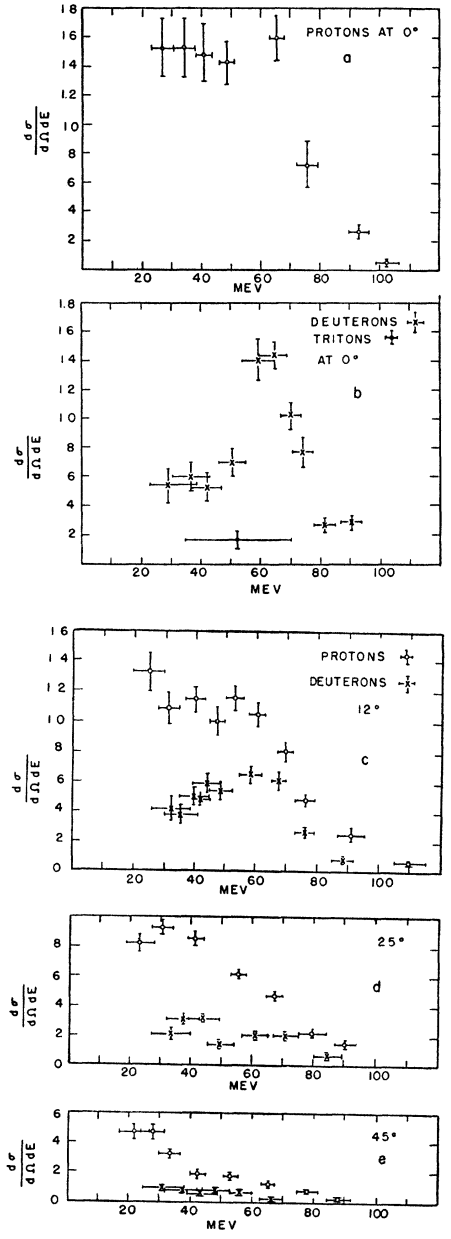

FIG. 7. Energy spectra of secondary particles from carbon $d\sigma/(d\Omega dE)$ in millibarns/steradian·Mev.

of 460 mg/cm² or more, it is necessary to make two assumptions about the values of the differential cross sections at angles other than the four at which they were measured.

In the first place, we have assumed that plots of differential cross section *vs.* angle would take the form of smooth curves passing through the measured points. Secondly, we have assumed that the cross sections for proton and for deuteron production are in the same ratio at angles greater than 45° as at the measured angles from 0° to 45°. The effect of the latter assumption on the final results is thought to be small, as the total cross sections are composed mostly of contributions from angles smaller than 45°; this can be seen by integration of the curves of Fig. 6, yielding the following values for the fraction of emitted particles falling in the range 0° to 45°:

Carbon	0.75
Copper	0.58
Lead	0.55.

By numerical integration of the quantities $d\sigma(E, \theta)/dEd\Omega$ over energy, we obtain the differential cross section

$$\left[\frac{d\sigma_p(\theta)}{d\Omega}\right]_{E>20\text{ Mev}} = \int_{E=20}^{\infty} \frac{d\sigma_p(E, \theta)}{d\Omega dE} dE$$

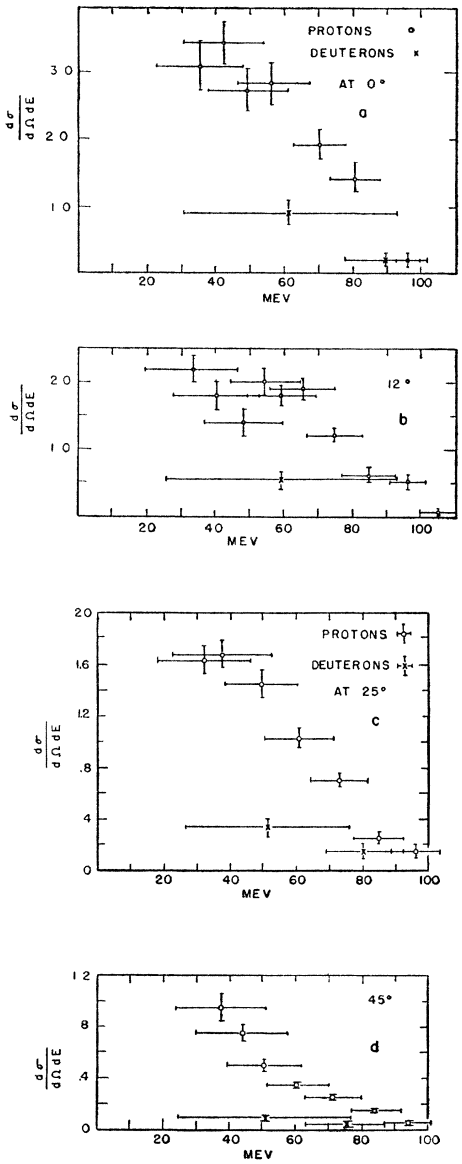

FIG. 8. Energy spectra of secondary particles from copper-$d\sigma/(d\Omega dE)$ in millibarns/steradian·Mev.

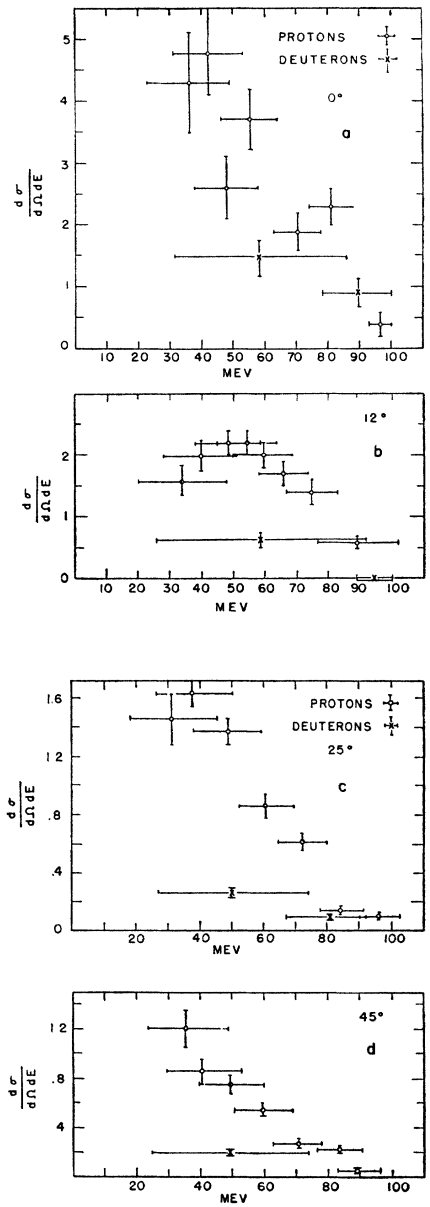

FIG. 9. Energy spectra of secondary particles from lead-$d\sigma/(d\Omega dE)$ in millibarns/steradian·Mev.

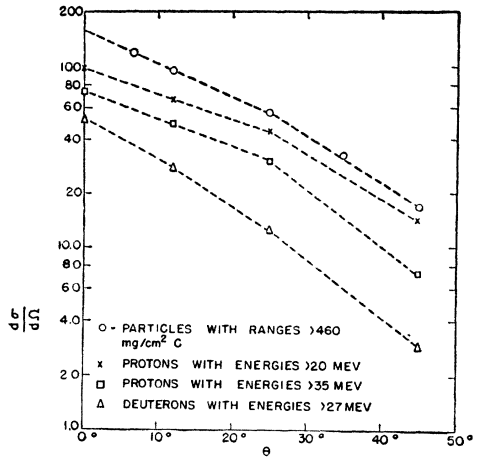

FIG. 10. Angular dependence of 90-Mev neutron-carbon cross sections for production of charged secondaries. $d\sigma/d\Omega$ in millibarns/steradian.

and the corresponding cross sections for protons above 35 Mev and for deuterons above 27 Mev plotted together with the quantities $\sum(\theta)$ in Figs. 10, 11, and 12.

By integrating appropriate parts of the curves in Figs. 10 to 12, Table I is derived. This table gives the total cross sections for producing the indicated particles within the indicated angular limits. The cross sections for producing deuterons between 45° and 180° (given in parentheses) are probable upper limits obtained by assuming the ratio between numbers of protons and deuterons found between 25° and 45° also holds from 45° to 180°. The corresponding proton cross section is then obtained by subtracting this deuteron cross section from the cross section for all particles, and is thus a lower limit.

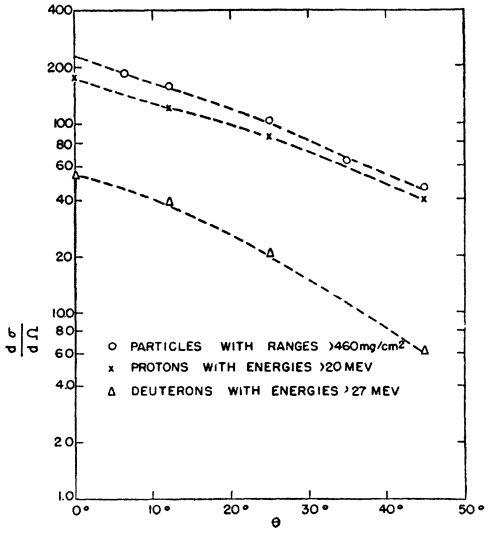

FIG. 11. Angular dependence of 90-Mev neutron-copper cross sections for production of charged secondaries. $d\sigma/d\Omega$ in millibarns/steradian.

VIII. DISCUSSION OF RESULTS

1. Shape of the Spectra

In the case of carbon, the only element for which there is much detailed information, the proton and deuteron spectra are seen to be fundamentally different. The proton spectrum at 0° is flat from 20 Mev to about 65 Mev, and then it decreases sharply as the energy increases further. While it is obviously impossible to deduce from this curve (Fig. 7) and the known neutron energy distribution (Fig. 3 of reference 17) the spectrum which would be obtained for monoenergetic neutrons, it may be worth while to point out the striking similarity of the observed curve to that derived from a rather simple assumption concerning the shape of the proton spectrum for such monoenergetic neutrons. For incident neutrons of energies of from 60 to 100 Mev, according to this assumption, the secondary proton spectrum in the forward direction is flat up to an energy equal to the neutron energy minus the energy required to make the reaction occur (about 15 Mev for 90-Mev neutrons) and then falls immediately to zero. On the basis of this assumption, the proton yield which would be obtained using neutrons with the energy distribution shown in Fig. 3 of reference 17 would be practically flat from 20 to 60 Mev, would fall to about one-half of the maximum value at 74 Mev, and to about one-eighth of that value at 90 Mev. All the values of the observed spectra at 0° and 12° fit such a distribution within the probable errors shown.

The deuteron energy distribution at 0° shows a peak at 60 to 65 Mev. The half-width of this peak is the same as the half-width of the neutron energy distribution, and the low energy tail is about twice as high relative to the peak as the low energy neutron tail is relative to the height of the neutron peak. This distribution fits the assumption that monoenergetic neutrons

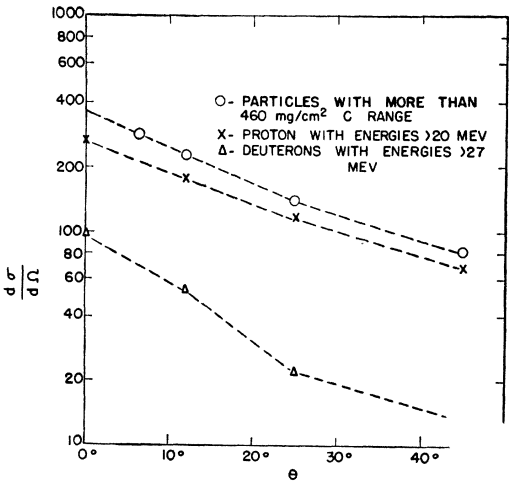

FIG. 12. Angular dependence of 90-Mev neutron sections for production of charged secondaries. $d\sigma/d\Omega$ millibarns/steradian.

would produce deuterons within a relatively narrow energy interval centered about 25 Mev below the neutron energy. As θ increases, the proton plateau and the deuteron peak both disappear. However, the average deuteron energy is higher than the average proton energy at all angles.

2. Total Cross Sections

The total cross sections for producing secondary protons of energy greater than 20 Mev are 0.090 barn for carbon, 0.24 barns for copper, and 0.42 barns for lead. The corresponding inelastic cross sections for 90-Mev neutrons as measured by DeJuren and Knable are 0.22, 0.78, and 1.79 barns. The ratios of these cross sections are 0.41 for carbon, 0.31 for copper, and 0.24 for lead. Since the cross section for striking at least one proton in the nucleus must be proportional to the inelastic cross section, the decrease in this ratio must be due to the increased difficulty which a proton has in leaving the larger nuclei.

For the case of carbon only, an additional total cross section is given, namely that for producing secondary protons of energy greater than 35 Mev. The reason for this particular choice of energy lies in the following arguments: In the $n-p$ scattering experiments performed at 90 Mev, the angular distribution of the scattered protons in the center-of-mass system is roughly symmetric about 90°. Consequently, in about one-half of the $n-p$ collisions the proton emerges with more than one-half of the energy of the incident neutron. Further, since the $n-p$ collision cross section is supposed to be three or four times larger than the $n-n$ cross section, about 0.8 of the inelastic cross section should produce $n-p$ collisions. If the nucleus were completely transparent, so that all struck protons could leave it without further collisions, we should expect that about 0.4 of the inelastic cross section would produce protons with more than half of the energy available to protons. Then since the maximum energy with which the proton can leave is about 70 Mev (taking 85 Mev as the mean energy of the impinging neutrons), the cross section for producing secondary protons with energies greater than 35 Mev would be about 0.4 of the inelastic cross section if the nucleus were completely transparent to the struck protons. In the case of carbon this would be about 100 millibarns. The observed cross section for this process is 52 millibarns, and hence about one-half of the protons leave without further interaction. The above arguments are too qualitative to allow a calculation of the mean free path, but the result is in agreement with the mean free paths estimated by Fernbach.

The total cross sections observed for deuteron production are given in Table I as 26 millibarns for carbon, 52 millibarns for copper, and 75 millibarns for lead. The ratios of these deuteron production cross sections to the inelastic cross sections are 0.12 for carbon, 0.067 for copper, and 0.042 for lead. Thus the deuteron production cross section, as well as the proton production cross section, increases more slowly with atomic number than does the inelastic cross section. The ratios of deuteron production cross section to proton production cross section are 0.29, 0.22, and 0.18 for carbon, copper, and lead respectively. This slower increase with Z of the deuteron cross section is to be expected, since in order for a deuteron to escape from a nucleus both of its component particles must escape without further interaction.

TABLE I. Total cross sections for the production of the particles indicated.*

	0°–25°	25°–45°	(0°–45°)	45°–180°	Total
Carbon					
All particles	48	39	87	30	117
All protons ($E>20$ Mev)	35	31	66	(24)	(90)
Protons ($E>35$ Mev)	24	19	43	(9)	(52)
All deuterons ($E>27$ Mev)	12	8	20	(6)	(26)
Copper					
All particles	88	82	170	123	293
Protons $E>20$ Mev	70	68	138	(103)	(241)
Deuterons $E>27$ Mev	18	14	32	(20)	(52)
Lead					
All particles	123	153	276	223	499
Protons $E>20$ Mev	100	132	232	(192)	(424)
Deuterons $E>27$ Mev	23	21	44	(31)	(75)

* All values are expressed in 10^{-27} cm².

3. The Origin of the Secondary Protons

An attempt was made by M. L. Goldberger[6] to predict the angular and energy distributions of the protons which would be ejected from heavy nuclei by 90-Mev neutrons. He used the Monte Carlo method, and treated the nucleus as a degenerate gas of nucleons. The experimentally determined $n-p$ differential cross sections were used to characterize the individual collisions which take place in the nucleus; the $n-n$ interactions were assumed to lead to the same angular distributions as in $n-p$ interactions, but with only one-fourth as large a total cross section. The angular distribution predicted by Goldberger gave a zero cross section for secondary particle production in the forward direction, and a maximum differential cross section at about 27°. The zero forward cross section was due to the action of the Pauli principle in forbidding small momentum transfers, which would leave one particle in a region of phase space already occupied by another particle.

The observed angular and energy distributions do not fit Goldberger's predictions. A possible explanation, suggested by R. Serber, for the lack of a minimum cross section in the forward direction is the following: The proton wave is refracted at the nuclear surface, since

the proton passes from a region in which there is a high negative potential to a region in which there is zero potential. The effect of this refraction then destroys completely any detailed structure such as that predicted around zero degrees.

The observed total cross section for producing secondary protons by bombardment of lead nuclei with 90-Mev neutrons is only about one-half of the predicted value. This indicates that the mean free path of particles in nuclear matter is smaller than the value given by Goldberger (6.2×10^{-13} cm) and is more nearly in agreement with that deduced by Fernbach *et al.*[5] (4.5×10^{-13} cm).

4. The Origin of the Secondary Deuterons

A possible mechanism for the origin of the secondary deuterons has been suggested by P. Cüer *et al.*[19] and by Chew and Goldberger,[20] and investigated in detail by the latter. This mechanism is characterized by a pick-up process, in which the impinging neutron combines with a proton from the nucleus to form a deuteron. Semiclassically, the process can be described as follows. Protons in the nucleus may have large components of momentum in the direction of the momentum of the impinging neutron. In fact, if the average kinetic energy of a bound nucleon is about 25 Mev, its root-mean-square momentum will be about one-half of the momentum of the impinging particle, and there may easily be nucleons present with momentum equal to that of the incident neutron. In such cases of high nucleon momentum, the nucleon and incident neutron may form a deuteron and so emerge from the nucleus. From this point of view, it would seem that the situation most likely to result in a secondary deuteron would be that in which the momenta of the proton and neutron were most nearly equal. However, for the case of equal momenta the deuteron would leave the nucleus with so much kinetic energy as to leave the nucleus in an impossibly low energy state. It can be seen qualitatively, though, that the energy of the deuteron would tend to be high, and that it would tend to emerge in the forward direction.

[19] Cüer, Morand, and Van Rossum, Comptes Rendus **228**, 481 (1949).

[20] G. F. Chew and M. L. Goldberger, Phys. Rev. **77**, 470 (1950).

5. Comparison to Other Experiments

Experimental investigations of some of the phenomena reported in this paper have also been made by Brueckner and Powell[11] and Bradner.[10] Brueckner and Powell have made a cloud chamber study of the angular and energy distributions of the particles emitted by carbon nuclei under bombardment with 90-Mev neutrons. Their method involved comparison of the $H\rho$'s of particles before and after passage through a plate of material of known stopping power. They found high energy protons, deuterons, and tritons, and their results are qualitatively in agreement with those obtained in the present experiment with respect to the ratios of number of protons to numbers of deuterons and tritons, and the general trends of the angular and energy distributions. There is a qualitative disagreement in the absolute values of the various cross sections, however, the values found in the present experiment being considerably larger than those determined in the cloud-chamber experiments.

Bradner's experiments used photographic plates, and were performed for the purpose of checking the existence of the secondary deuterons. The method involved a comparison of the grain density of tracks with a given residual range. The ratio of protons to deuterons in the forward direction as determined by his experiments is in agreement with that found in the present experiment.

The authors wish to express their gratitude to Professor Segrè and the other members of the committee who guided this research, for their frequent advice and encouragement. Thanks are also due Professor E. O. Lawrence and Dr. B. J. Moyer for their continued interest in this work; to Mr. Clyde Wiegand for the loan of equipment and for numerous suggestions; to Professor Serber, Dr. Chew, and Dr. Goldberger for many interesting discussions of the theoretical implications of this work; and to the cyclotron operating crew, especially Mr. Vale and Mr. Watt, who kindly supplied about 10^{12} high energy neutrons.